1 **Air Quality and Climate Change, Topic 3 of the Model Inter-Comparison**

2 **Study for Asia Phase III (MICS-Asia III), Part II: aerosol radiative effects**

3 **and aerosol feedbacks**

4 Meng Gao[1], Zhiwei Han[2,3], Zhining Tao[4,5], Jiawei Li[2,3], Jeong-Eon Kang[6], Kan Huang[7], Xinyi

5 Dong[8], Bingliang Zhuang[9], Shu Li[9], Baozhu Ge[10], Qizhong Wu[11], Hyo-Jung Lee[6], Cheol-Hee

6 Kim[6], Joshua S. Fu[8], Tijian Wang[9], Mian Chin[5], Meng Li[12], Jung-Hun Woo[13], Qiang Zhang[14],

7 Yafang Cheng[12], Zifa Wang[4,10], Gregory R. Carmichael[15]

8

9 1 Department of Geography, Hong Kong Baptist University, Hong Kong SAR, China
10 2 Key Laboratory of Regional Climate-Environment for Temperate East Asia, Institute of
11 Atmospheric Physics, Chinese Academy of Sciences, Beijing, China
12 3 University of Chinese Academy of Sciences, Beijing 100049, China
13 4 Universities Space Research Association, Columbia, MD, USA
14 5 NASA Goddard Space Flight Center, Greenbelt, MD, USA
15 6 Department of Atmospheric Sciences, Pusan National University, Busan, South Korea
16 7 Department of Environmental Science and Engineering, Fudan University, Shanghai, China
17 8 Department of Civil and Environmental Engineering, University of Tennessee, Knoxville,
18 TN, USA
19 9 School of Atmospheric Sciences, Nanjing University, Nanjing, China
20 10 State Key Laboratory of Atmospheric Boundary Layer Physics and Atmospheric Chemistry,
21 Institute of Atmospheric Physics, Chinese Academy of Sciences, Beijing, China
22 11 College of Global Change and Earth System Science, Beijing Normal University, Beijing,
23 China
24 12 Multiphase Chemistry Department, Max Planck Institute for Chemistry, Mainz, Germany
25 13 Department of Advanced Technology Fusion, Konkuk University, Seoul, South Korea
26 14 Ministry of Education Key Laboratory for Earth System Modeling, Center for Earth System
27 Science, Tsinghua 15 University, Beijing, China
28 15 Center for Global and Regional Environmental Research, University of Iowa, Iowa City,
29 IA, USA
30 Correspondence to: M. Gao (mmgao2@hkbu.edu.hk), Z. Han (hzw@mail.iap.ac.cn), and G. R.
31 Carmichael (gcarmich@engineering.uiowa.edu)

32

33

34

35

36

Abstract

Topic 3 of the Model Inter-Comparison Study for Asia (MICS-Asia) Phase III examines how online coupled air quality models perform in simulating high aerosol pollution in the North China Plain region during wintertime haze events and evaluates the importance of aerosol radiative and microphysical feedbacks. This paper discusses the estimates of aerosol radiative forcing, aerosol feedbacks, and possible causes for the differences among the models. Over the Beijing-Tianjin-Hebei (BTH) region, the ensemble mean of aerosol direct radiative forcing (ADRF) at the top of atmosphere, inside the atmosphere and at the surface are -1.9, 8.4 and -10.3 W/m^2, respectively. Subdivisions of direct and indirect aerosol radiative forcing confirm the dominant roles of direct forcing. During severe haze days (January 17-19, 2010), the averaged reduction in near surface temperature for the BTH region can reach 0.3-3.0 °C. The responses of wind speeds at 10 m (WS10) inferred from different models show consistent declines in eastern China. For the BTH region, aerosol-radiation feedback induced changes in PM$_{2.5}$ range from 6.0 to 8.8 µg/m^3 ($< 6.6\%$). Sensitivity simulations indicate the most sensitive parameter for aerosol radiative forcing and feedback is the aerosol mixing state, and BC exhibits large contribution to atmospheric heating although it accounts for a small share of mass concentration of PM$_{2.5}$.

1 Introduction

Aerosols change weather and climate via the following pathways: they absorb and scatter solar and thermal radiation to alter the radiative balance of the earth-atmosphere system, which is referred to as direct effects; and, they serve as cloud condensation nuclei (CCN) and/or ice nuclei (IN) to modify cloud properties, which is referred to as indirect effects (*Haywood and Boucher, 2000*). The suppression of cloud convection induced by direct effects of absorbing aerosols is called the semi-direct effect (*Lohmann and Feichter, 2005*). Increases in cloud droplet number can increase cloud albedo for a constant liquid water path (LWP), which is further classified as the first indirect effect or Twomey effect (*Twomey, 1991*). More but smaller cloud droplets reduce precipitation intensity but increase cloud lifetime, which is called cloud lifetime or second indirect aerosol effect (*Albrecht, 1989*). In turn, changes in the radiative

Atmospheric
Chemistry
and Physics
Discussions

66   balance can alter meteorological variables (e.g. temperature, relative humidity, photolysis rate,

67   etc.) and further the transport, diffusion and chemical conversion of trace gases and aerosols,

68   while changes in clouds can affect in-cloud aqueous-phase chemistry and wet deposition of

69   gases and aerosols.

70   The impacts of meteorology on chemistry have been explicitly treated in chemical transport

71   models (CTMs). For example, temperature modulates chemical reaction and photolysis rates,

72   affects volatility of chemical species, and biogenic emissions, wind speed and direction

73   determine transport and mixing, and precipitation influences wet deposition (*Baklanov et al.,*

74   *2014*). However, due to the complexity of these processes and lack of computational resources,

75   the influences of atmospheric compositions on weather and climate have been generally

76   ignored in previous CTMs (*Baklanov et al., 2014*). Until recently, with the rapid development

77   of coupled meteorology and chemistry models, many new studies have been conducted to

78   investigate the aerosol direct and indirect effects and feedbacks (*Baklanov et al., 2017; Forkel*

79   *et al., 2015; Gao et al., 2016, 2017*; *Han et al., 2010; Huang et al., 2016; Jacobson et al., 2007;*

80   *Wang et al., 2014; Zhang et al., 2010*). In highly polluted regions like Asia, aerosol feedbacks

81   can be particularly important (*Gao et al., 2016, 2017*).

82   Aerosol feedbacks during haze events in China have been explored using multiple online

83   coupled meteorology-chemistry models, including WRF-Chem (the Weather Research

84   Forecasting model coupled with Chemistry, *Gao et al., 2016, 2017*), WRF-CMAQ

85   (Community Multiscale Air Quality, *Wang et al., 2014*). Nevertheless, large uncertainties

86   remain in the modelling of these processes, due to the lack of direct observational constraints

87   and challenges in predicting aerosol compositions. Thus, the inter-comparison of coupled

88   meteorology-chemistry models is of great significance to better understand the differences,

89   causes, and uncertainties within these processes.

90   Topic 3: air quality and climate change within the Model Inter-Comparison Study for Asia

91   Phase III (MICS-Asia phase III) was initialized to address these issues (*Gao et al., 2018a*).

92   Results from seven applications of fully online coupled meteorology-chemistry models using

93   harmonized emission and chemical boundary conditions were submitted to this topic (*Gao et*

94   *al., 2018a*). These model applications include two applications of WRF-Chem by different

95   institutions, two applications of the National Aeronautics and Space Administration (NASA)

96   Unified WRF (NU-WRF) model with different model resolutions, one application of the

97   Regional Integrated Environment Modeling System with Chemistry (RIEMS-Chem, *Han et al.,*

98   *2010*), one application of the coupled Regional Climate Chemistry Modeling System

99   (RegCCMS), and one application of the coupled WRF-CMAQ model (*Gao et al., 2018a*). More

100   detailed information of the participating models, how the experiments were designed and

101   model evaluations have been archived in *Gao et al. (2018a)*. In this paper, we analyze the

102   results from the participating models to address the following questions: (1) how large is the

103   aerosol radiative forcing during winter haze in China and how differently are models estimating

104   it? (2) to what extend do aerosol feedbacks change meteorological variables? and how

105   differently are current models estimating these changes? (3) to what extent do aerosol

106   feedbacks contribute to the evolution of high aerosol concentrations during winter haze

107   episodes and what are the best estimates from different models? And (4) what are the major

108   causes of the differences among the models? Sect. 2 presents the estimates of aerosol direct

109   radiative forcing inferred from multiple models, including the separation of direct and indirect

110   effects. In Sect. 2, we discuss the impacts of aerosol-radiation feedbacks on meteorological

111   variables and $PM_{2.5}$ concentrations. Sect. 4 illustrates the sensitivity of aerosol forcing to

112   different processes in the model, and the summary is presented in Sect. 5.

113

114   **2 Aerosol Direct and Indirect Forcing**

115   **Fig. 1** shows the monthly mean all-sky aerosol direct radiative forcing (ADRF) over China.

116   The spatial distributions of ADRF at the surface and inside the atmosphere inferred from

117   multiple models are generally consistent, with the largest values in eastern and southwestern

118   China. Over the BTH region, M5 and M7 reports the highest ADRF at the surface (-16.7 and -

119   17.0 W/m^2), and the greatest ADRF inside the atmosphere (10.1 and 14.6 W/m^2) (**Table 1**).

120   M6 shows the lowest ADRF both at the surface and inside the atmosphere (-3.6 and 3.6 W/m^2)

121   (**Table 1**). It is noticed that M6 predicts lower AOD than M5 and M7 (*Gao et al., 2018a*),

122   which could partly explain the weaker ADRF, and M6 also use an external assumption which

123   likely cause weaker absorption and ADRF in the atmosphere. However, the reported ADRF at

124   the top of the atmosphere (TOA) vary widely, and no consensus is reached on whether the

125   forcing is positive or negative. The spatial pattern of ADRF at the TOA inferred from M5 are

126   consistently negative across the modeling domain, while the results inferred from other models

127   are patchy with positive values to the north or to the southwest (**Fig. 1**). Over the BTH region,

128   suggested ADRF at the TOA range from -7.6 to 0.2 W/m^2 (**Table 1**). *Li et al. (2010)* reported

129   observation-based estimates of aerosol radiative forcing across China to be 0.3±1.6 at the TOA.

130   *Chung et al. (2005)* and *Chung et al. (2010)* estimated the forcing over south Asia to be -2.9

131   W/m^2 and -3.6 W/m^2 at the TOA, respectively. The magnitudes of modelled estimated aerosol

132   radiative forcing values are generally in line with estimates inferred from observations, while

133   discrepancies among models could be resulted from assumptions for mixing state and other

134   model treatments. The discussions on how different model treatments affect the results of

135   ADRF is provided in Sect. 4.

136   **Fig. 2** exhibits the ensemble mean of monthly averaged ADRF at the TOA, inside the

137   atmosphere and at the surface. Elevated forcing inside the atmosphere and at the surface are

138   mainly located in east China. However, the ensemble mean of forcing at the TOA over the

139   ocean is slightly higher than that over the land. Over the BTH region, the ensemble mean of

140   ADRF at the TOA, inside the atmosphere and at the surface are -1.9, 8.4 and -10.3 W/m^2,

141   respectively. When only haze days are considered, these values increase to -2.4, 19.0 and -21.4

142   W/m^2, respectively. In winter, the aerosol radiative forcing in China is largely contributed by

143   the power sector and residential sector, but with different signs of the contribution (*Gao et al.,*

144   *2018b*).

145   M4 and M5 further provide subdivision of direct and indirect aerosol radiative forcing. As

146   listed in **Table 2**, although the magnitudes of forcing estimated by M4 and M5 differ from each

147   other, the dominant roles of direct forcing are consistent. Over north China and during

148   wintertime, aerosol indirect forcing is negligible due to the lack of water vapor the stable

149   weather conditions.

150

3 Impact of aerosol feedback on meteorological variables and PM$_{2.5}$

concentrations

153   Here we analyze results for simulations on the time period, January 2010, of a heavy haze event.

154   When extreme haze events happen, high aerosol loadings can reduce significantly the

155   shortwave radiation reaching the surface, modifying near-surface temperature (*Gao et al.,*

156   *2017*). **Fig. 3** displays the aerosol-radiation feedback induced changes in temperature at 2 m

157   (T2) from M1 (a), M2 (b), M4 (c), M5 (d), M6 (e), M7 (f) (M1: Pusan National University;

158   M2: University of Iowa; M4: NASA; M5: Institute of Atmospheric Physics; M6: Nanjing

159   University; M7: University of Tennessee; *Gao et al., 2018a*). All models show reductions in

160   T2, but the magnitudes differ. M5 exhibits the largest areas where T2 is reduced, which include

161   northeastern China, while significant reduction in T2 inferred from other models are mainly

162   concentrated in southern China (**Fig. 3**). In Beijing, the monthly averaged reductions in T2

163   from multiple models range from 0-1℃, with the greatest changes calculated from M5 (**Table**

164   **1**). In the Beijing-Tianjin-Hebei (BTH) region, similar magnitudes (0-1.3 ℃) are found. When

165   only severe haze days (January 17-19) are considered, the averaged reduction in T2 for Beijing

166   (0.1-3.2 ℃) and the BTH region (0.3-3.0 ℃) are further enhanced (**Table 3**). In terms of

167   aerosol-radiation feedback induced temperature reduction, M1 and M2 generally report similar

168   magnitudes, which are lower than M4, M5 and M7. Model evaluation of $PM_{2.5}$ composition in

169   *Gao et al. (2018a)* reveals that M4 overpredicts strong scattering organic carbon, which could

170   be one of the reasons for higher temperature reduction.

171   Pronounced decreases in water vapor at 2 m (Q2) are mostly located in southern China (**Fig.**

172   **4**), where water vapor is more abundant due to the proximity to the sea. During extreme haze

173   days, the aerosol-radiation feedback induced decreases in Q2 in the BTH region from multiple

174   models range from 0.07 to 0.5 g/kg, with the lowest estimate from M1 and the highest from

175   M6 (**Table 3**). The responses of wind speeds at 10 m (WS10) inferred from different models

176   are generally consistent, displaying decreases in eastern China except M6. In the BTH region,

177   the monthly mean aerosol-radiation feedback induced decreases in WS10 range from 0.02 to

178   0.09 m/s (**Table 1**), and more pronounced reductions are suggested by M4, M5 and M7 (**Fig.**

179   **5**).

180   Because of aerosol-radiation feedback, most models report that surface $PM_{2.5}$ concentrations

181   are generally enhanced in China, with the exception of M6 (**Fig. 6**). It is also noteworthy that

182     $PM_{2.5}$ concentrations decrease in the Gobi desert and Taklimakan desert of western China in

183   M5 and M2, which is caused by the decreased wind speed near the surface due to the weakened

184   downward transport of momentum from upper layer above boundary layer to the surface (*Han*

185   *et al., 2013*). For M6 the increases are patchy over east China, with decreases to the north and

186   to the southwest. The monthly mean $PM_{2.5}$ are enhanced by 0.1-1.4 µg/m^3 for Beijing, and by

187   0.8-4.4 µg/m^3 for the BTH region. The enhancement fractions are generally below 2.7% for

188   Beijing, and below 7.8% for the BTH region (**Table 1**). To further understand how aerosol-

189   radiation feedback contribute to the formation of haze event, we calculate the mean increase

190   for extreme haze days (January 17-19). For the BTH region, the contribution of aerosol-

191   radiation feedback to $PM_{2.5}$ concentrations are lower than 6%, and the enhancement are below

192   8.5 µg/m^3. *Gao et al. (2017)* demonstrates that the aerosol-radiation feedback induced changes

193   in $PM_{2.5}$ are negligible during nighttime, so we further calculate daytime mean changes, as

194   listed in **Table 3**. For the BTH region, M2 reports the highest enhancement (12.9 µg/m^3) of

195     $PM_{2.5}$ concentrations during daytime. Except M6, other models report similar magnitudes of

196   the enhancement, ranging from 6.0 to 8.8 µg/m^3. The enhancement fraction is still not more

197   than 6.6% for the BTH region, and below 8.3% for Beijing. **Table 3** also displays the maximum

198   enhancement of $PM_{2.5}$ for the BTH region. M7 suggests the largest $PM_{2.5}$ enhancement (up to

199   60.9 µg/m^3), followed by M2 (up to 55.4 µg/m^3), and M5 (41.2 µg/m^3). Other three models,

200   M1, M4 and M6 indicate the aerosol-radiation induced increase in $PM_{2.5}$ can reach up to more

201   than 20 µg/m^3 in the BTH region (**Table 3**).

202   These results can be compared to previous studies. The contributions of aerosol-radiation

203   feedback to haze formation in China have been investigated in many previous studies (*Ding et*

204   *al., 2016; Gao et al., 2015; Gao et al., 2016; Liu et al., 2018; J. Wang et al., 2014; Z. Wang et*

205   *al., 2014; Wang et al., 2015; Wu et al., 2019; Zhang et al., 2015; Zhang et al., 2018; Zhong et*

206   *al., 2018*), but the reported values partly diverge. *Ding et al. (2016)*, *J. Wang et al. (2014)* and

207   *Zhong et al. (2018)* indicate that the aerosol radiative effects can increase $PM_{2.5}$ by more than

208   100 µg/m^3 or +70%. *Gao et al. (2015), Z. Wang et al. (2014), Wang et al. (2015),* and *Zhang et*

209   *al. (2018)* suggest that the contributions are generally within the range of 10-30%. These

210   studies are different from ours in terms of time period, region, emissions and resulting aerosol

211   levels. For example, the monthly mean $PM_{2.5}$ level in January 2010 are about 50% lower than

212   that in January 2013. The above studies also differed in the assumptions and treatments for

213   aerosol properties and mixing state. According to the results from multiple models in this study,

214 the contribution of aerosol-radiation feedback to haze formation during this time period are

215 generally below 10%.   Uncertainties remain resulting from the errors in simulated chemical

216 compositions (*Gao et al., 2018a*). As suggested in model evaluation, sulfate and organic

217 aerosol concentrations are generally underestimated by most models in this study, except that

218 M4 overestimate organic aerosol (*Gao et al., 2018a*). These were attributed to the missing

219 multiphase oxidation mechanisms of SO_2, and different secondary organic aerosol (SOA)

220 formation mechanisms in these models (*Gao et al., 2018a*).

221

222 4 Sensitivity to Different Processes

223 To further explore the causes for the differences among models and the main factors influencing

224 the aerosol-radiation feedback, several sensitivity simulations were conducted using the

225 RIEMS-Chem model (M5) focusing on the effects of aerosols mixing state, hygroscopic

226 growth, black carbon and mineral dust.

227

228 4.1 Aerosol mixing state

229 A simulation was run with the assumption of external mixing (results discussed above applied

230 the assumption of internal mixing), and the corresponding results are displayed in **Fig. 7-9**. The

231 simulation with the assumption of external mixing shows weaker (30% smaller) ADRF at the

232 surface, TOA and in the atmosphere (**Fig. 9a, 9f and 9k**), resulting in smaller changes in surface

233 meteorological variables and $PM_{2.5}$ concentrations (**Fig. 8a, 8d, 8g, and 8j**). For example, the

234 monthly mean maximum changes in air temperature, relative humidity, wind speed and $PM_{2.5}$

235 values are -2.7°C, +3%, -0.24m/s and 16 $\mu g\ m^{-3}$, respectively in the southern Huabei province

236 from the simulation with internal mixing, whereas the corresponding changes from external

237 mixing assumption are -1.4°C, +2%, -0.12m/s and 8 $\mu g\ m^{-3}$, respectively. These differences

238 demonstrate the significant impact of aerosol mixing state on the ADRF and the aerosol-

239 radiation feedback. It should also be emphasized that the aerosol mixing state can vary with

240 time and location. Some previous measurements in the Huabei Plain exhibit that aerosols are

241 partially internally mixed and the fraction of internal mixing could be increasing from clean to

242 haze period (*Li et al., 2014*).

243

244 4.2 Hygroscopic growth

245 Given the important effect of aerosol hygroscopic growth on ADRF (*Li et al., 2014*), another

246 simulation was conducted with decreased relative humidity by FNL nudging above boundary

247 layer. Such perturbation of RH was based on the fact that M5 predicted higher relative humidity

248 (water vapor mixing ratio) than the observations (*Gao et al., 2017*). The simulation with

249 reduced RH produces lower values of AOD (**Fig. 7f**) and ADRF (**Fig. 9e, 9j, and 9o**, about 10%

250 lower) because of the decreased relative humidity and weaker hygroscopic growth.

251

252 4.3 Soil dust

253 M5 includes all anthropogenic aerosols and dust, sea salt, while the other models except M2

254 do not consider natural dust. A simulation with dust aerosol excluded was conducted and the

255 results show the dust aerosol contributes to total $PM_{2.5}$ concentration and ADRF in parts of

256 central and northeast China, especially in the middle reaches of the Yellow River with the

257 ADRF by dust at the surface contribute up to -6 W m^{-2} in terms of monthly mean (**Fig. 9d, 9l,**

258 **and 9n**), which indicates the nonnegligible role of dust even in winter. Both the overprediction

259 of relative humidity (water vapor) and the inclusion of mineral dust can partly explain the

260 relatively stronger ADRF from M5 compared with other models.

261

262 4.4 The effect of BC

263 To identify the effect of BC, two simulations without BC and with doubled BC concentrations

264 were conducted. When BC is not included, the ADRF in the atmosphere decreases largely (**Fig.**

265 **9g**), indicating the strong absorbing effect of BC. The ADRF at the surface changes by about

266 10% (**Fig. 9b**). The monthly mean maximum changes in air temperature, relative humidity,

267 wind speed and $PM_{2.5}$ values in this case are -2.2°C, +3.5%, -0.18m/s and 10 μg m^{-3},

268 respectively, in the southern Huabei region. When BC concentrations are doubled, the

269 corresponding values are -3.0°C, +2.0%, -0.27m/s and 18 μg m^{-3}, respectively. The comparison

270 with the changes in the base case (the corresponding values are -2.7°C, +3%, -0.24m/s and 16

271 μg m^{-3}, respectively) indicates that the effect of BC is smaller than that due to other scattering

272 aerosols (inorganic and organic aerosols), and the percentage contribution by BC to the total

273 feedback could be in a range of 20-30%. It is also found that the effect of BC under internal

274 mixing condition is larger than that under external mixing. Gao et al. (2016) demonstrates that

275 the impacts of BC on meteorology and $PM_{2.5}$ can account for as high as 60% of the total aerosol

276 feedbacks, although it is not of great significance in terms of mass concentration.

277   The above sensitivity simulations suggest the importance of mixing state assumption for

278 ADRF and feedback and the potentially dominant role of scattering aerosols over absorbing

279 aerosols in aerosol radiative effect during haze periods.

280

5 Summary

282 Topic 3 of MICS-Asia III focuses on understanding how current online coupled air quality

283 models perform in capturing extreme aerosol pollution event in northern China and how

284 aerosols interact with radiation and weather. Seven applications of different online coupled

285 meteorology-chemistry models were involved in this activity. Previous paper has demonstrated

286 that main features of the accumulation of air pollutants are generally well represented, while

287 large differences in the models were found in the predicted $PM_{2.5}$ chemical compositions (*Gao*

288 *et al., 2018a*). These inconsistency would lead to differences in estimated ADRF and aerosol

289 feedbacks.

290 The spatial distributions of ADRF at the surface and inside the atmosphere inferred from

291 multiple models are generally consistent, while the spatial pattern of ADRF at the TOA greatly

292 differ. Over the BTH region, the ensemble mean of ADRF at the TOA, inside the atmosphere

293 and at the surface are -1.9, 8.4 and -10.3 W/m^2, respectively. Subdivisions of direct and indirect

294 aerosol radiative forcing confirm the dominant roles of direct forcing.

295 During severe haze days (January 17-19), the averaged reduction in T2 for the BTH region

296 can reach 0.3-3.0 °C. The responses of wind speeds at 10 m (WS10) inferred from different

297 models show consistent declines in eastern China. For the BTH region, aerosol-radiation

298 feedback induced changes in $PM_{2.5}$ range from 6.0 to 8.8 $\mu g/m^3$ (< 6.6%). Our findings differ

299 from previous studies in terms of time period, region and emissions, for example, the monthly

300 mean $PM_{2.5}$ level in January 2010 are about 50% lower than that in January 2013.

301 Sensitivity simulations were conducted using the RIEMS-Chem model (M5) to understand the

Atmospheric
Chemistry
and Physics
Discussions

302   influences of aerosols mixing state, hygroscopic growth, black carbon and mineral dust. The

303   results indicate the most sensitive parameter for ADRF and feedback is the aerosol mixing state,

304   and BC exhibits large contribution to atmospheric heating although it accounts for a small share

305   of mass concentration of $PM_{2.5}$.

306

307   **Author Contributions**

308   M.G., Z.H., and G.R.C. designed the study, and M.G. processed and analyzed the data. M.G.,

309   Z.H., and G.R.C. wrote the paper with inputs from all other authors.

310

311   **Data availability**

312   The measurements and model simulations data can be accessed through contacting the

313   corresponding authors.

314

315   **Competing interests**

316   The authors declare that they have no conflict of interests.

317

318   **Acknowledgement**

321
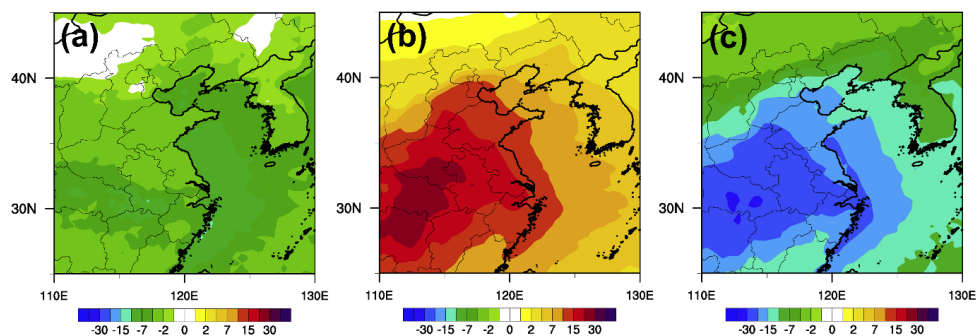
322

323

324
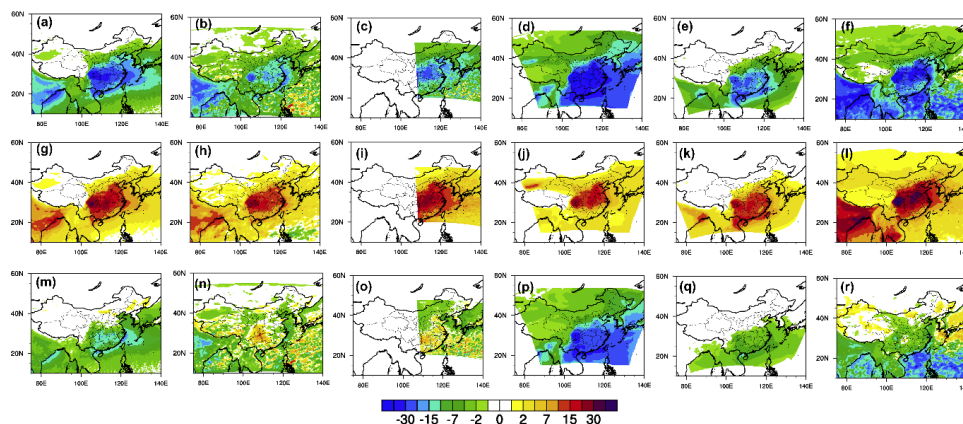
Figure 1. Monthly mean aerosol direct radiative forcing at the surface, inside the atmosphere and at the top of the atmosphere inferred from M1 (a, g, m), M2 (b, h, n), M4 (c, i, o), M5 (d, j, p), M6 (e, k, q), M7 (f, l, r) (M1: Pusan National University; M2: University of Iowa; M4: NASA; M5: Institute of Atmospheric Physics; M6: Nanjing University; M7: University of Tennessee; *Gao et al., 2018*)
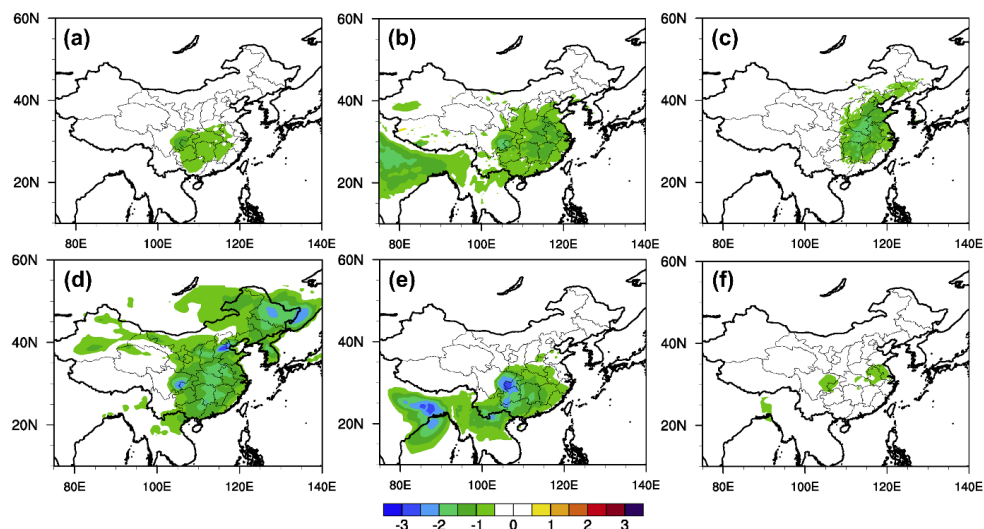

331

Figure 2. Ensemble mean of monthly mean aerosol direct radiative forcing at the top of the atmosphere (a), inside the atmosphere (b) and at the surface (c)
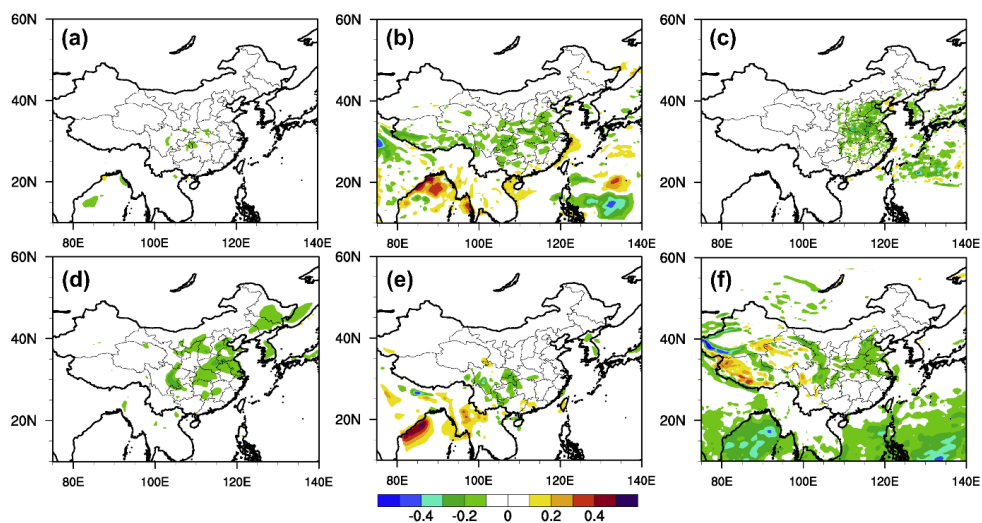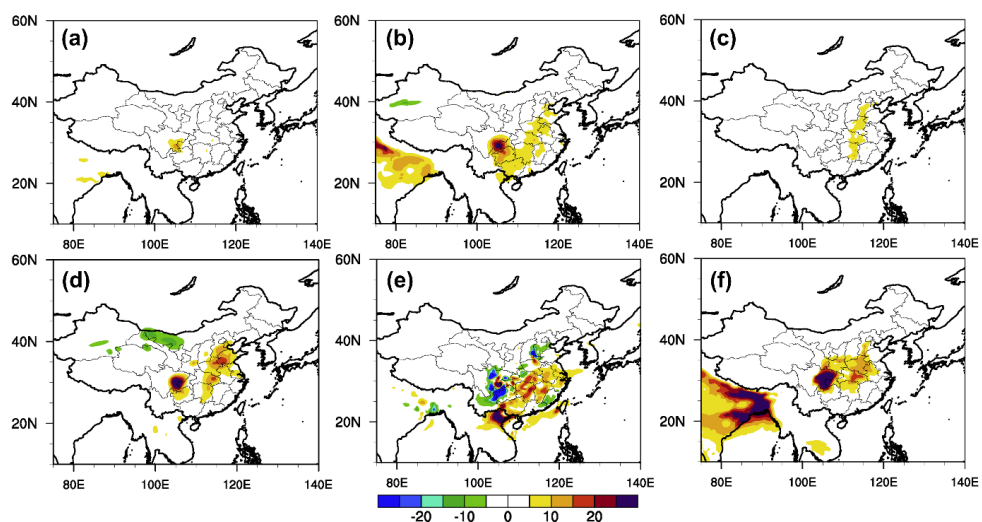
334

335

Figure 3. Monthly mean changes in temperature at 2 m (T2, ºC) due to aerosol radiative effects from M1 (a), M2 (b), M4 (c), M5 (d), M6 (e), M7 (f) (M1: Pusan National University; M2: University of Iowa; M4: NASA; M5: Institute of Atmospheric Physics; M6: Nanjing University; M7: University of Tennessee; *Gao et al., 2018*)
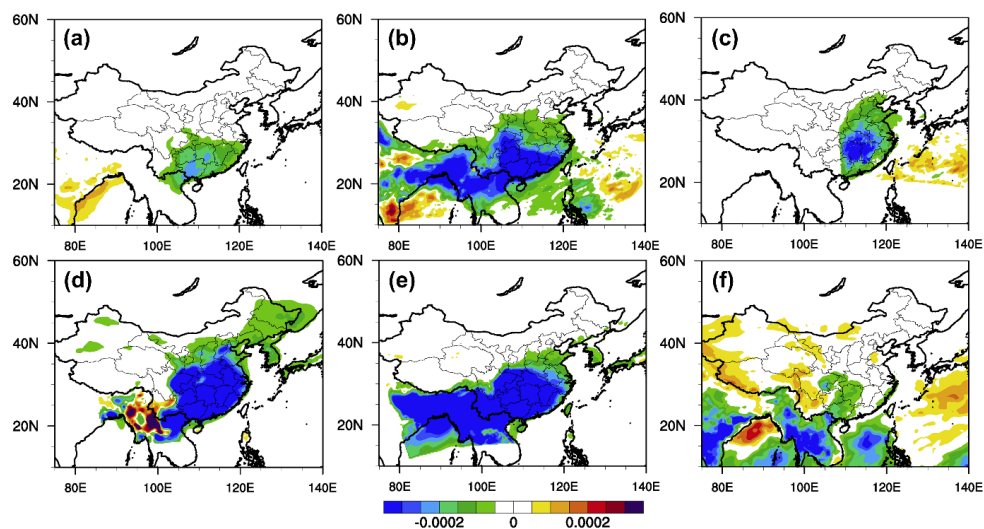
Figure 4. Monthly mean changes in water vapor at 2 m (Q2, kg/kg) due to aerosol radiative effects from M1 (a), M2 (b), M4 (c), M5 (d), M6 (e), M7 (f) (M1: Pusan National University; M2: University of Iowa; M4: NASA; M5: Institute of Atmospheric Physics; M6: Nanjing University; M7: University of Tennessee; *Gao et al., 2018*)

13

Atmospheric
Chemistry
and Physics
Discussions

Figure 5. Monthly mean changes in wind speeds at 10 m (WS10, m/s) due to aerosol radiative effects from M1 (a), M2 (b), M4 (c), M5 (d), M6 (e), M7 (f) (M1: Pusan National University; M2: University of Iowa; M4: NASA; M5: Institute of Atmospheric Physics; M6: Nanjing University; M7: University of Tennessee; *Gao et al., 2018*)
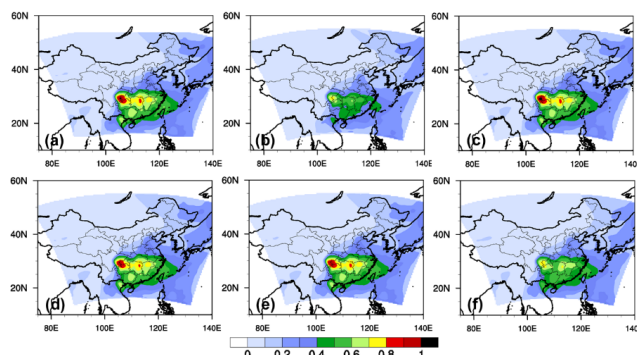

Figure 6. Monthly mean changes in surface $PM_{2.5}$ ($\mu g/m^3$) due to aerosol radiative effects from M1 (a), M2 (b), M4 (c), M5 (d), M6 (e), M7 (f) (M1: Pusan National University; M2: University of Iowa; M4: NASA; M5: Institute of Atmospheric Physics; M6: Nanjing University; M7: University of Tennessee; *Gao et al., 2018*)
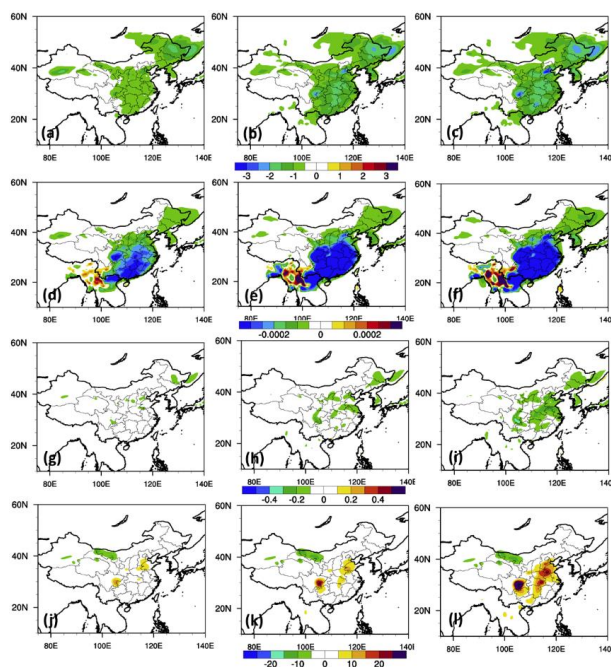
360

361

362 Figure 7. Monthly mean RIEMS-Chem modeled AOD from different simulations: control run
363 (default simulation with internal mixing assumption) (a), external mixing assumption (b),
364 internal mixing assumption but without BC (c), internal mixing assumption but with doubled
365 BC (d), without dust and sea-salt (e), and reduced RH (f)

366

367

368 Figure 8. Monthly mean RIEMS-Chem modeled changes in T2 (ºC), Q2 (kg/kg), WS10 (m/s)
369 and PM$_{2.5}$ (μg/m^3) from different simulations: external mixing assumption (first column),
370 internal mixing assumption but without BC (second column) and internal mixing assumption
371 but with doubled BC (third column)

372

373
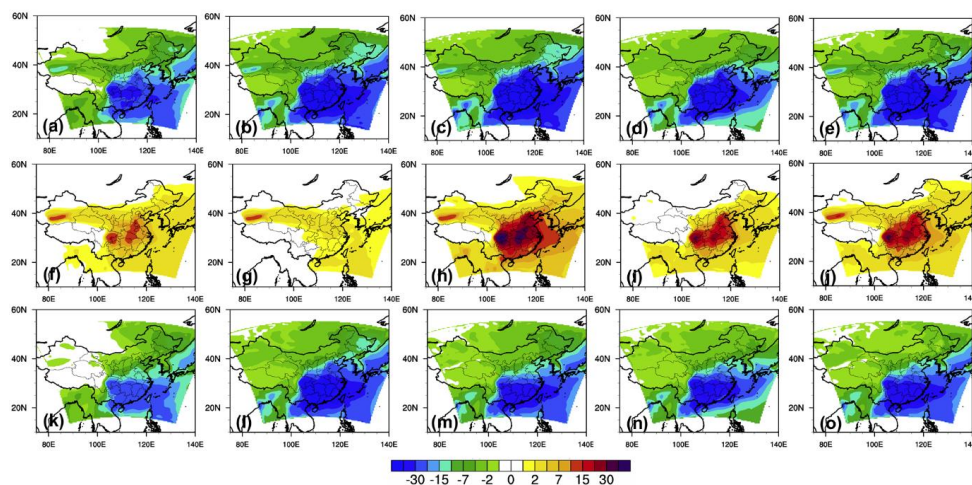
Figure 9. Monthly mean RIEMS-Chem modeled aerosol direct radiative forcing at the surface (a-e), inside the atmosphere (f-j) and at the top of the atmosphere (k-o) from different simulations: external mixing assumption (first column), internal mixing assumption but without BC (second column), internal mixing assumption but with doubled BC (third column), without dust and sea-salt (fourth column), and reduced RH (fifth column)

374
375
376
377
378
379
380
381
382
383
384
385
386
387
388
389
390
391
392
393
394
395
396
397
398
399
400
401
402

Atmospheric
Chemistry
and Physics
Discussions

403   Table1 Monthly Mean Aerosol Direct Radiative Forcing (W/m^2) and Changes in T2 (ºC), Q2

404   (g/kg), WS10 (0.1 m/s), and PM$_{2.5}$ (µg/m^3) for Beijing and Beijing-Tianjin-Hebei region

Beijing	M1 PNU	M2 UIOWA	M4 NASA	M5 IAP	M6 NJU	M7 UTK
ADRF TOA	-0.6	-2.2	-0.8	-5.1	-0.1	-2.5
ADRF ATM	5.8	4.3	9.3	7.1	2.4	11.6
ADRF SFC	-6.4	-6.5	-10.1	-12.2	-2.5	-14.1
T2	-0.1	-0.3	-0.7	-1.0	-0.1	0.0
Q2	-1.2E-2	-2.3E-2	-6.4E-2	-1.1E-1	-5.8E-3	2.1E-2
WS10	-0.2	-0.2	-0.6	-0.3	0.0	-1.2
PM$_{2.5}$	0.1 (0.2%)	1.4 (1.6%)	1.1 (1.7%)	1.2 (2.7%)	-1.2 (-2.2%)	1.0 (1.4%)
BTH						
ADRF TOA	0.2	-1.4	-0.3	-7.6	0.0	-2.4
ADRF ATM	7.3	5.4	10.1	9.1	3.6	14.6
ADRF SFC	-7.1	-6.8	-10.4	-16.7	-3.6	-17.0
T2	-0.2	-0.4	-0.8	-1.3	-0.2	0.0
Q2	-1.0E-2	-2.5E-2	-8.1E-2	-1.6E-1	-2.9E-2	2.5E-2
WS10	-0.2	-0.2	-0.9	-0.7	0.1	-0.9
PM$_{2.5}$	0.8 (1.4%)	1.8 (1.8%)	2.2 (3.2 %)	4.4 (7.8%)	-4.2 (-5.7%)	2.2 (2.4%)

405

406   Table 2 Monthly Mean Aerosol Direct Radiative Forcing and indirect Radiative Forcing

407   (W/m^2) at the top of the atmosphere inferred from M4 and M5

Beijing	direct	Indirect
M4	-0.77	-0.15
M5	-5.05	-0.01
BTH		
M4	-0.28	0.1
M5	-7.63	-0.04

408

409

410

411

412

413

414

415 Table 3 Mean Aerosol Direct Radiative Forcing (W/m^2) and Changes in T2 (ºC), Q2 (g/kg),
416 WS10 (0.1 m/s), and PM$_{2.5}$ (µg/m^3) for Beijing and Beijing-Tianjin-Hebei (BTH) region
417 averaged over January 17-19 2010

Beijing	M1 PNU	M2 UIOWA	M4 NASA	M5 IAP	M6 NJU	M7 UTK
ADRF TOA	2.6	-1.4	1.8	-11.9	-0.6	-3.3
ADRF ATM	18.6	9.8	21.5	19.0	7.3	32.3
ADRF SFC	-16.0	-11.2	-19.7	-30.8	-7.9	-35.6
T2	-0.5	-0.5	-1.7	-3.2	-0.1	-1.5
Q2	-7.4E-2	-6.2E-2	-2.6E-1	-4.5E-1	-1.3E-2	-9.2E-2
WS10	-0.1	0.2	-2.3	1.7	0.5	-0.8
PM$_{2.5}$	-1.1 (-0.9%)	3.8 (1.7%)	6.3 (3.8%)	-2.6 (-2.1%)	-7.9 (-4.7%)	1.3 (1.1%)
BTH						
ADRF TOA	1.4	0.1	4.9	-16.0	-0.7	-3.8
ADRF ATM	18.3	12.0	19.1	18.7	10.0	36.1
ADRF SFC	-16.9	-11.9	-14.2	-34.6	-10.7	-39.9
T2	-0.6	-0.7	-1.6	-3.0	-0.3	-1.5
Q2	-7.1E-2	-8.2E-2	-2.9E-1	-5.0E-1	-1.2E-1	-8.9E-2
WS10	-0.3	-0.4	-2.5	0.5	0.3	-0.9
PM$_{2.5}$	2.9 (2.3%)	8.5 (3.7%)	5.3 (3.9%)	7.9 (5.9%)	-10.5 (-6.2%)	5.1 (2.7%)
Daytime PM$_{2.5}$						
Beijing	2.4 (2.0%)	8.5 (3.9%)	8.4 (5.5%)	-2.1 (-1.8%)	-4.2 (-3.2%)	10.7 (8.3%)
BTH	6.0 (4.9%)	12.9 (5.9%)	6.6 (5.2%)	8.8 (6.6%)	-6.2 (-3.8%)	6.4 (3.8%)
	Up to 26.4	Up to 55.4	Up to 26.5	Up to 41.2	Up to 22.8	Up to 60.9

418

419

420

421

422

423

References:

Albrecht, B.A.: Aerosols, cloud microphysics, and fractional cloudiness, Science, 245(4923), pp.1227-1230, https://doi.org/10.1126/science.245.4923.1227, 1989.

Haywood, J., and Boucher, O.: Estimates of the direct and indirect radiative forcing due to tropospheric aerosols: A review, Rev. geophy., 38(4), pp.513-543, https://doi.org/10.1029/1999rg000078, 2000.

Baklanov, A., Schlünzen, K., Suppan, P., Baldasano, J., Brunner, D., Aksoyoglu, S., Carmichael, G., Douros, J., Flemming, J., Forkel, R. and Galmarini, S.: Online coupled regional meteorology chemistry models in Europe: current status and prospects, Atmos. Chem. Phys., 14(1), pp.317-398, https://doi.org/10.5194/acpd-13-12541-2013, 2014.

Baklanov, A., Brunner, D., Carmichael, G., Flemming, J., Freitas, S., Gauss, M., Hov, Ø., Mathur, R., Schlünzen, K.H., Seigneur, C. and Vogel, B.: Key Issues for Seamless Integrated Chemistry–Meteorology Modeling, Bull. Amer. Meteo. Soc., 98(11), pp.2285-2292, https://doi.org/10.1175/bams-d-15-00166.1, 2017.

Chung, C.E., Ramanathan, V., Kim, D. and Podgorny, I.A.: Global anthropogenic aerosol direct forcing derived from satellite and ground-based observations, Jour. Geophy. Res.: Atmos., 110(D24), https://doi.org/10.1029/2005jd006356, 2005.

Chung, C.E., Ramanathan, V., Carmichael, G., Kulkarni, S., Tang, Y., Adhikary, B., Leung, L.R. and Qian, Y.: Anthropogenic aerosol radiative forcing in Asia derived from regional models with atmospheric and aerosol data assimilation, Atmos. Chem. Phys., 10(13), pp.6007-6024, https://doi.org/10.5194/acpd-10-821-2010, 2010.

Ding, A.J., Huang, X., Nie, W., Sun, J.N., Kerminen, V.M., Petäjä, T., Su, H., Cheng, Y.F., Yang, X.Q., Wang, M.H. and Chi, X.G.: Enhanced haze pollution by black carbon in megacities in China, Geophy. Res. Let., 43(6), pp.2873-2879, https://doi.org/10.1002/2016gl067745, 2016.

Forkel, R., Balzarini, A., Baró, R., Bianconi, R., Curci, G., Jiménez-Guerrero, P., Hirtl, M., Honzak, L., Lorenz, C., Im, U. and Pérez, J.L.: Analysis of the WRF-Chem contributions to AQMEII phase 2 with respect to aerosol radiative feedbacks on meteorology and pollutant distributions, Atmos. Env., 115, pp.630-645, https://doi.org/10.1016/j.atmosenv.2014.10.056, 2015.

Gao, Y., Zhang, M., Liu, Z., Wang, L., Wang, P., Xia, X., Tao, M. and Zhu, L.: Modeling the feedback between aerosol and meteorological variables in the atmospheric boundary layer during a severe fog–haze event over the North China Plain, Atmos. Chem. Phys., 15(8), pp.4279-4295, https://doi.org/10.5194/acpd-15-1093-2015, 2015.

Gao, M., Carmichael, G.R., Wang, Y., Saide, P.E., Yu, M., Xin, J., Liu, Z. and Wang, Z.: Modeling study of the 2010 regional haze event in the North China Plain, Atmos. Chem. Phys., 16(3), p.1673, https://doi.org/10.5194/acpd-15-22781-2015, 2016.

Gao, M., Carmichael, G.R., Wang, Y., Saide, P.E., Liu, Z., Xin, J., Shan, Y. and Wang, Z.: Chemical and Meteorological Feedbacks in the Formation of Intense Haze Events, In Air Pollution in Eastern Asia: An Integrated Perspective (pp. 437-452), Springer, Cham., https://doi.org/10.1007/978-3-319-59489-7_21, 2017.

Gao, M., Han, Z., Liu, Z., Li, M., Xin, J., Tao, Z., Li, J., Kang, J.E., Huang, K., Dong, X. and Zhuang, B.: Air quality and climate change, Topic 3 of the Model Inter-Comparison Study for Asia Phase III (MICS-Asia III)–Part 1: Overview and model evaluation. Atmos. Chem.

468   Phys., 18(7), p.4859, https://doi.org/10.5194/acp-18-4859-2018, 2018a.

469 Gao, M., Ji, D., Liang, F. and Liu, Y.: Attribution of aerosol direct radiative forcing in China
470   and India to emitting sectors, Atmos. Env., 190, pp.35-42,
471   https://doi.org/10.1016/j.atmosenv.2018.07.011, 2018b.

472 Han, Z.: Direct radiative effect of aerosols over East Asia with a regional coupled
473   climate/chemistry model, Meteorologische Zeitschrift, 19(3), pp.287-298,
474   https://doi.org/10.1127/0941-2948/2010/0461, 2010.

475 Han, Z., Li, J., Guo, W., Xiong, Z., and Zhang, W.: A study of dust radiative feedback on
476   dust cycle and meteorology over East Asia by a coupled regional climate-chemistry-
477   aerosol model, Atmos. Environ., 68, 54–63,
478   https://doi.org/10.1016/j.atmosenv.2012.11.032, 2013.

479 Huang, X., Ding, A., Liu, L., Liu, Q., Ding, K., Niu, X., Nie, W., Xu, Z., Chi, X., Wang, M.
480   and Sun, J.: Effects of aerosol-radiation interaction on precipitation during biomass-
481   burning season in East China, Atmos. Chem. Phys., 16(15), https://doi.org/10.5194/acp-
482   2016-272, 2016.

483 Jacobson, M.Z., Kaufman, Y.J. and Rudich, Y.: Examining feedbacks of aerosols to urban
484   climate with a model that treats 3-D clouds with aerosol inclusions, Jour. Geophy. Res.:
485   Atmos., 112(D24), https://doi.org/10.1029/2007jd008922, 2017.

486 Li, J., Han, Z., and Zhang, R.: Influence of aerosol hygroscopic growth parameterization on
487   aerosol optical depth and direct radiative forcing over East Asia, Atmos. Res., 140-141,
488   14-27, https://doi.org/10.1016/j.atmosres.2014.01.013, 2014.

489 Li, Z., Lee, K.H., Wang, Y., Xin, J. and Hao, W.M.: First observation-based estimates of cloud-
490   free aerosol radiative forcing across China, Jour. Geophy. Res.: Atmos., 115(D7),
491   https://doi.org/10.1029/2009jd013306, 2010.

492 Liu, Q., Jia, X., Quan, J., Li, J., Li, X., Wu, Y., Chen, D., Wang, Z. and Liu, Y.: New positive
493   feedback mechanism between boundary layer meteorology and secondary aerosol
494   formation during severe haze events, Sci. rep., 8(1), p.6095,
495   https://doi.org/10.1038/s41598-018-24366-3, 2018.

496 Lohmann, U. and Feichter, J.: Global indirect aerosol effects: a review, Atmos. Chem.
497   Phys., 5(3), pp.715-737, https://doi.org/10.5194/acp-5-715-2005, 2005.

498 Twomey, S.: Aerosols, clouds and radiation. Atmospheric Environment. Part A. General
499   Topics, 25(11), pp.2435-2442, https://doi.org/10.1016/0960-1686(91)90159-5, 1991.

500 Wang, H., Xue, M., Zhang, X.Y., Liu, H.L., Zhou, C.H., Tan, S.C., Che, H.Z., Chen, B. and
501   Li, T.: Mesoscale modeling study of the interactions between aerosols and PBL
502   meteorology during a haze episode in Jing–Jin–Ji (China) and its nearby surrounding
503   region–Part 1: Aerosol distributions and meteorological features, Atmos. Chem.
504   Phys., 15(6), pp.3257-3275, https://doi.org/10.5194/acp-15-3257-2015, 2015.

505 Wang, J., Wang, S., Jiang, J., Ding, A., Zheng, M., Zhao, B., Wong, D.C., Zhou, W., Zheng,
506   G., Wang, L. and Pleim, J.E.: Impact of aerosol–meteorology interactions on fine particle
507   pollution during China's severe haze episode in January 2013, Env. Res. Let., 9(9),
508   p.094002, https://doi.org/10.1088/1748-9326/9/9/094002, 2014.

509 Wang, Z., Li, J., Wang, Z., Yang, W., Tang, X., Ge, B., Yan, P., Zhu, L., Chen, X., Chen, H.
510   and Wand, W.: Modeling study of regional severe hazes over mid-eastern China in January
511   2013 and its implications on pollution prevention and control, Sci. China Earth

512   Sciences, 57(1), pp.3-13, https://doi.org/10.1007/s11430-013-4793-0, 2014.

513   Wu, J., Bei, N., Hu, B., Liu, S., Zhou, M., Wang, Q., Li, X., Liu, L., Feng, T., Liu, Z., Wang,
514   Y., Cao, J., Tie, X., Wang, J., Molina, L. T., and Li, G.: Aerosol-radiation feedback
515   deteriorates the wintertime haze in North China Plain, Atmos. Chem. Phys. Discuss.,
516   https://doi.org/10.5194/acp-2018-1288, in review, https://doi.org/10.5194/acp-19-8703-
517   2019, 2019.

518   Zhang, B., Wang, Y. and Hao, J.: Simulating aerosol–radiation–cloud feedbacks on
519   meteorology and air quality over eastern China under severe haze conditions in
520   winter, Atmos. Chem. Phys., 15(5), pp.2387-2404, https://doi.org/10.5194/acp-15-2387-
521   2015, 2015.

522   Zhang, X., Zhang, Q., Hong, C., Zheng, Y., Geng, G., Tong, D., Zhang, Y. and Zhang, X.:
523   Enhancement of PM2. 5 Concentrations by Aerosol-Meteorology Interactions Over
524   China, Jour. Geophy. Res.: Atmos., 123(2), pp.1179-1194,
525   https://doi.org/10.1002/2017jd027524, 2018.

526   Zhang, Y., Wen, X.Y. and Jang, C.J.: Simulating chemistry–aerosol–cloud–radiation–climate
527   feedbacks over the continental US using the online-coupled Weather Research Forecasting
528   Model with chemistry (WRF/Chem), Atmos. Env., 44(29), pp.3568-3582,
529   https://doi.org/10.1016/j.atmosenv.2010.05.056, 2010.

530   Zhong, J., Zhang, X., Dong, Y., Wang, Y., Liu, C., Wang, J., Zhang, Y. and Che, H.: Feedback
531   effects of boundary-layer meteorological factors on cumulative explosive growth of PM
532   2.5 during winter heavy pollution episodes in Beijing from 2013 to 2016, Atmos. Chem.
533   Phys., p.247, https://doi.org/10.5194/acp-18-247-2018, 2018.

534

535

536

537

538

539